Supplement of Hydrol. Earth Syst. Sci., 20, 209–225, 2016
http://www.hydrol-earth-syst-sci.net/20/209/2016/
doi:10.5194/hess-20-209-2016-supplement

Hydrology and Earth System Sciences
Open Access
EGU

Supplement of

Differences in the water-balance components of four lakes in the southern-central Tibetan Plateau

S. Biskop et al.

Correspondence to: S. Biskop (sophie.biskop@uni-jena.de)

Supplementary Material

1 Supplemental Figures

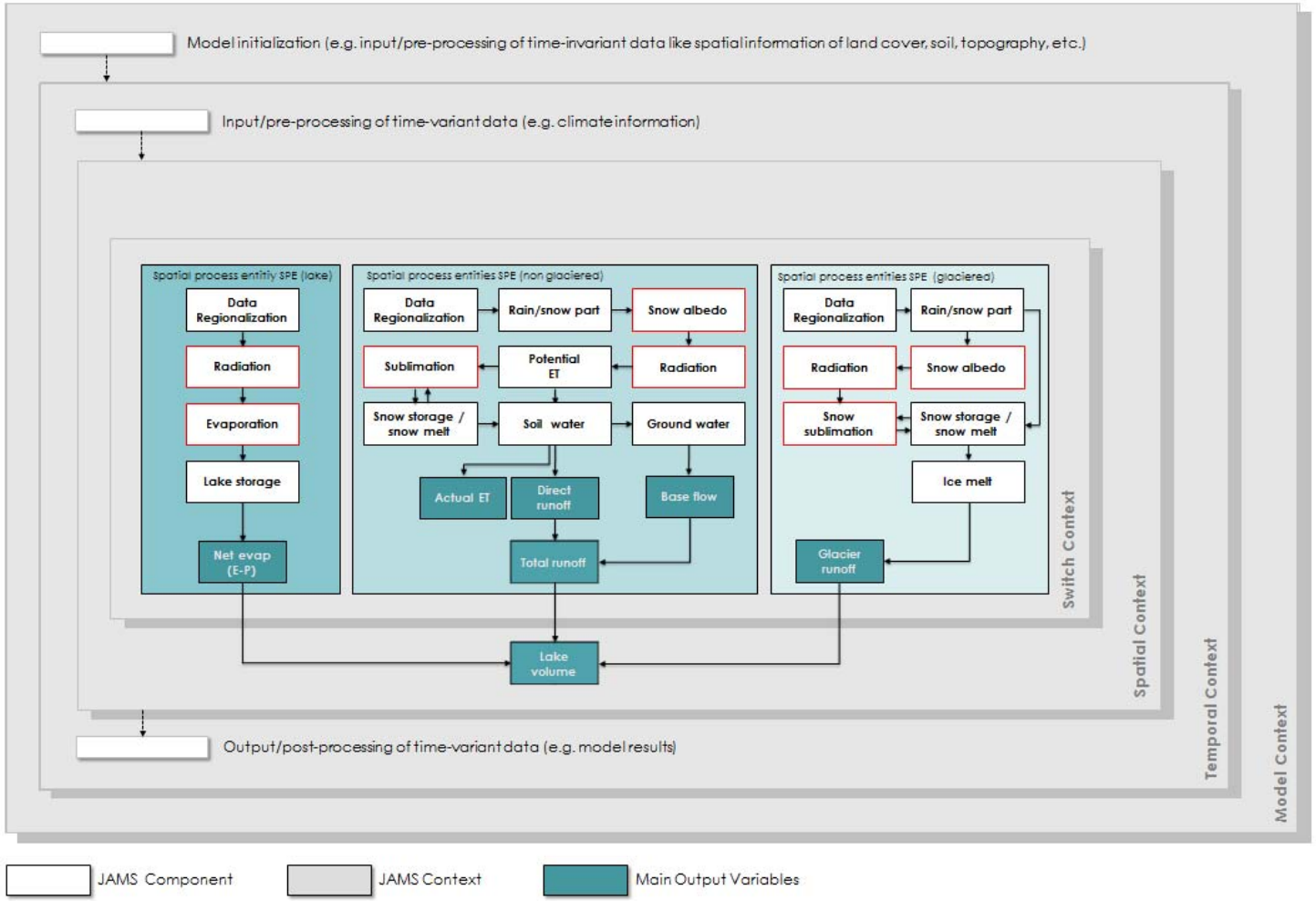

Figure S1: Simplified illustration of the model layout including components and context components within the Jena Adaptable Modelling System (JAMS) framework. Modified or new components are indicated in red.

2 Supplemental Tables

Table S1: Model parameters.

Parameter	Description	Value	Reference / note
Precipitation distribution			
Snow_trs	Threshold temperature for 50% rain, 50% snow fall [°C]	3.75	a
Snow_trans	Half width of the transition range within which both precipitation forms occur [°C]	2.75	a
PSF	Precipitation-scaling factor	0.5-0.8	b
Snow module			
snowCritDens	Critical density of snow pack	0.381	Nepal et al. (2014)
snowColdContent	Cold content of snow pack	0.0012	Nepal et al. (2014)
t_factor	Melt factor by sensible heat	2.84	Nepal et al. (2014)
r_factor	Melt factor by liquid precipitation	0.21	Nepal et al. (2014)
g_factor	Melt factor by soil heat flow	3.73	Nepal et al. (2014)
baseTemp	Threshold temperature for snow melt [°C]	0	default value
Glacier module			
MeltFactorIce	Melt factor for ice	2.5	Nepal et al. (2014)
AlphaIce	Radiation melt factor for ice	0.001	Schulla (2012)
tbase	Threshold temperature for ice melt [°C]	0	default value
Soil module			
AWCA	Available water capacity adaption (multiplier)	1	default value
ETR	Linear evapotranspiration-reduction factor	0.6	default value
LVD	Lateral vertical runoff distribution	1	default value
Ground water module			
GWK	Retention coefficient	180	default value

a: The upper and lower threshold for precipitation phase corresponds to 6.5°C and 1°C according to Mölg et al. (2014). b: In several basins the precipitation-scaling factor corresponds to: 0.80 (Nam Co), 0.75 (Tangra Yumco), 0.85 (Paiku Co), 0.50 (Mapam Yumco).

3 Supplemental Model Description

Regionalization of meteorological data

The regionalization module, which is used for the interpolation of the HAR10 raster points (centroid of the raster cell) to each HRU unit, is based on the Inverse Distance Weighting (IDW) method. To account for horizontal and vertical climate variability, the regionalization procedure within the Jena Adaptable Modelling System (JAMS) provides the opportunity to combine distance weighting with an optional elevation correction. In this study the four nearest raster points were taken into account for the regionalization of the meteorological input data. All data sets, except air temperature, were regionalized using only IDW. In the case of air temperature, the elevation correction was done when the coefficient of determination (r^2) was equal or greater 0.75 (default value). However in glacier areas where HAR data grid points are often lacking, the temperature lapse rate of 0.7°C/100 m (Huintjes, 2014) has been applied to transfer the temperature values of the closest raster points to the particular glacier-HRU. The simple temperature lapse-rate method implemented in JAMS is described by Nepal (2012). For the transfer of precipitation values to the HRUs, no lapse rate has been considered due to the high spatial heterogeneity of precipitation distribution and the lack of reliable precipitation lapse rate information.

Net Radiation

Within JAMS, net radiation is calculated following the Food and Agriculture Organization of the United Nations (FAO) proposed use of the Penman-Monteith model (Allen et al., 1998). For a detailed description of the net radiation calculation it is referred to the FAO Irrigation and Drainage Paper No. 56 (hereafter referred to as FAO56) (Allen et al., 1998). Because in the standard radiation module of JAMS an albedo change during periods of snow cover is not considered, a new component was implemented for the estimation of snow albedo for time steps if the snow water equivalent is greater than zero. The ageing curve of the albedo of freshly fallen snow is calculated according to Rohrer (1992).

For the calculation of the net long-wave radiation (R_{nl}) Yin et al. (2008) tested three formulas, including FAO56 (Allen et al., 1998), FAO24 (Doorenboos and Pruitt, 1977) and Penman (Penman, 1948) for the special high altitude conditions on the TP. The comparison with observed R_{nl} at sites throughout the TP has indicated that the Perman's empirical model had the highest accuracy. The R_{nl} simualtions using the FAO24 and FAO56 models consistently underestimated the observations. As a consequence, the potential evapotranspiration would be overestimated if the FAO56 model is used without modification on the TP (Yin et al., 2008). Thus, the Penman simulation method, combined with the minimum and maximum temperature, was recommended by Yin et al. (2008) to calculate R_{nl} for conditions applicable to the TP. With regard to this, the longwave radiation part of the FAO56 calculation was modified according to the recommendations of Yin et al. (2008).

In the standard radiation module of JAMS, there is no distinction between the calculations for the net long-wave radiation for land versus water surfaces. Due to the fact that the exchange of radiant energy between the lake surface and the atmosphere in the form of long-wave (thermal) radiation is significant for large lakes, a new component for the calculation of the net long wave radiation over lakes (R_{nl}) that takes into account water surface temperature was implemented in JAMS. The long-wave radiation fluxes are calculated according to the Stefan-Boltzmann law. The incident long-wave

atmospheric radiation at the water surface that is available to the water body after reflection is determined by the air temperature and the effective emissivity of the atmosphere. The thermal radiation emitted by the water surface depends on water-surface temperature and on the emissivity of water. The commonly used nomenclature for calculating the amount of the net long-wave radiation over water surface (e.g., Jensen, 2010) was implemented in JAMS. Regarding the calculation of effective emissivity of the atmosphere the formulation incorporating the Brutsaert (1975) clear-sky parameterization and the Deardorff (1978) cloudiness correction was used in this study.

Evapotranspiration

Within the framework of JAMS, the physically-based Penman-Monteith model is implemented, in accordance with the FAO56 report (Allen et al. 1998). A detailed description of the entire calculation procedure can be found in the FAO56 guideline of Allen et al. (1998) or in Nepal (2012). For the estimation of open-water evaporation rates from large lakes, the Penman equation modified by with the addition of an empirical estimation of the lake heat storage (Jensen et al., 2005) was used. Due to the lack of lake-temperature depth profiles, the energy storage change in the lake is estimated, based upon the net short-wave and long-wave radiation and using the empirical formulation given in Jensen et al. (2005). As suggested by Valiantzas (2006), the reduced wind function proposed by Linacre (1993) was applied for the estimation of evaporation from large open-water body surfaces.

Snow processes and ice melt

In order to calculate the daily snow-accumulation rate, the fraction of the total precipitation that falls as snow is estimated previously in a sub module of JAMS. The separation between solid and liquid precipitation phase, thereby, depends on the following: i) a defined threshold temperature T_{rs} (in °C) which conforms to the temperature where 50% of precipitation is falling as snow and 50% as rain and ii) a transition parameter T_{trans} (in K) that is taken as the half width of the transition range within which both precipitation forms occur. Within JAMS, the user can choose between a snow module based on a simple day-degree approach or a more complex calculation method that is principally following the approach developed by Knauf (1980). Due to the high importance of the refreezing process in the snow pack in the study region, the latter module that combines empirical or conceptual approaches with more physically-based routines was selected for use in this study. The complex snow module takes into account the phases of snow accumulation, snow ablation and the compaction of the snow pack caused by snowmelt or rain on the snow pack. It includes the calculation of different state variables, such as snow-water equivalent, snow density, snow depth, snow age, etc. For a more detailed description, reference is made to Nepal (2012).

Snowmelt processes on the glacier surface are calculated according to the approach described previously. If the entire snow cover of a glacier HRU has melted (i.e. the snow-water equivalent is equal to zero) and the threshold temperature for melt, as defined by the user, is lower than the air temperature, the ice-melt rate is calculated according to the extended temperature-index approach (Hock, 1999) that has been successfully used in other studies (e.g., Zhang et al., 2007; Huss et al., 2008; Nepal et al., 2014).

Soil-water budget and runoff processes

Due to a lack of detailed soil information in the study area, the simple soil-water module of J2000g described in Krause and Hanisch (2009) is used to fill this data gap. The soil module consists of a simple water storage (i.e. middle-pore storage (MPS)) that regulates the relation between evapotranspiration and direct runoff and groundwater recharge. The maximum soil-water storage capacity (maxMPS) is defined from the available water capacity (AWC) of the specific soil type within the respective modeling unit. During the process of model calibration, the storage-capacity values of all modeling units can be increased or decreased by using a multiplicative calibration parameter (AWCA) with the same value for all modeling units (Krause and Hanisch, 2009).

The MPS is filled by precipitation and snowmelt until the maxMPS is reached. The amount of water which exceeds the maximum soil-water storage capacity will be used initially for evapotranspiration. In case that the potential evapotranspiration rate is greater than the inflow, the MPS is "emptied" (e.g., lost to the atmosphere) by evapotranspiration. The water loss from the MPS through evapotranspiration is controlled by the actual soil-water saturation (actMPS), the potential evapotranspiration and a linear evapotranspiration-reduction factor (ETR). The calibration coefficient ETR has a range of values between 0 and 1 and defines a specific threshold of the actMPS which triggers a linear reduction of the potential evapotranspiration rate if actMPS falls below this threshold (Krause and Hanisch, 2009).

Runoff is generated only when the soil-water storage is saturated. Excess water which is not allocated to evapotranspiration is allocated into either direct runoff or percolation, based upon the slope and the maximum percolation rate of any given HRU and the calibration parameter LVD (Lateral vertical runoff distribution). The percolation component is transferred to a groundwater-storage component, where the outflow is computed based on a linear-storage approach and a specific-retention coefficient (GWK) (Krause and Hanisch, 2009). According to other studies (e.g., Lei et al., 2013), the effects of upwelling groundwater derived from fault zones and lake-groundwater exchange on the water balance are assumed to be negligible. The total runoff of the non-glaciated land surface occurs, based upon the summation of the direct runoff and the base-flow components from the respective HRUs.

References

Allen, R. G., Pereira, L. S., Raes, D. and Smith, M.: Crop evapotranspiration: Guidelines for computing crop water requirements. FAO Irrigation and drainage paper 56, Rome, Italy, 1998.

Brutsaert, W.: On a Derivable Formula for Long-Wave Radiation From Clear Skies, Water Resour. Res., 11(5), 742–744, 1975.

Deardorff, J. W.: Efficient prediction of ground surface temperature and moisture, with inclusion of a layer of vegetation, J. Geophys. Res., 83(C4), 1889–1903, 1978.

Doorenboos, J. and Pruitt, W. O.: Guidelines for predicting crop water requirements. FAO irrigation and drainage paper 24, Rome, Italy, 1977.

Hock, R.: A distributed temperature-index ice- and snowmelt model including potential direct solar radiation, J. Glaciol., 45(149), 101–111, 1999.

Huintjes, E.: Energy and mass balance modelling for glaciers on the Tibetan Plateau - Extension, validation and application of a coupled snow and energy balance model, Dissertation, RWTH Aachen, 2014.

Huss, M., Farinotti, D., Bauder, A. and Funk, M.: Modelling runoff from highly glacierized alpine drainage basins in a changing climate, Hydrol. Process., 22, 3888–3902, 2008.

Jensen, M., Dotan, A. and Sanford, R.: Penman-Monteith Estimates of Reservoir Evaporation, in Impacts of Global Climate Change, pp. 1–24, American Society of Civil Engineers., 2005.

Jensen, M. E.: Estimating evaporation from water surfaces. Presented at the CSU/ARS Evapotranspiration Workshop, Fort Collins, Colorado, USA, 2010 (Available from: http://ccc.atmos.colostate.edu/ET_Workshop/ET_Jensen/ET_water_surf.pdf).

Knauf, D.: Die Berechnung des Abflusses aus einer Schneedecke, Schriftenr. des Dtsch. Verbandes für Wasserwirtschaft und Kult., 46, 97–135, 1980.

Krause, P. and Hanisch, S.: Simulation and analysis of the impact of projected climate change on the spatially distributed waterbalance in Thuringia, Germany, Adv. Geosci., 21, 33–48, 2009.

Lei, Y., Yao, T., Bird, B. W., Yang, K., Zhai, J. and Sheng, Y.: Coherent lake growth on the central Tibetan Plateau since the 1970s: Characterization and attribution, J. Hydrol., 483, 61–67, 2013.

Linacre, E. T.: Data-sparse estimation of lake evaporation, using a simplified Penman equation, Agric. For. Meteorol., 64, 237–256, 1993.

Nepal, S.: Evaluating Upstream-Downstream Linkages of Hydrological Dynamics in the Himalayan Region, Dissertation, FSU Jena, 2012.

Nepal, S., Krause, P., Flügel, W.-A., Fink, M. and Fischer, C.: Understanding the hydrological system dynamics of a glaciated alpine catchment in the Himalayan region using the J2000 hydrological model, Hydrol. Process., 28(3), 1329–1344, 2014.

Penman, H. L.: Natural evaporation from open water, bare and grass, Proc. Roy. Soc. London, A, 193(1032), 120–145, 1948.

Rohrer, M. B.: Die Schneedecke im Schweizer Alpenraum und ihre Modellierung. Analyse langjähriger Schneemessungen und Modellierung des Wasseräquivalentes aufgrund zeitlich hoch aufgelöster operationell gemessener meteorologischer Daten, Züricher Geogr. Schriften, 49, 178, 1992.

Valiantzas, J. D.: Simplified versions for the Penman evaporation equation using routine weather data, J. Hydrol., 331(3-4), 690–702, 2006.

Yin, Y., Wu, S., Zheng, D. and Yang, Q.: Radiation calibration of FAO56 Penman-Monteith model to estimate reference crop evapotranspiration in China, Agric. Water Manag., 95, 77–84, 2008.

Zhang, Y., Liu, S., Xu, J. and Shangguan, D.: Glacier change and glacier runoff variation in the Tuotuo River basin, the source region of Yangtze River in western China, Environ. Geol., 56(1), 59–68, 2007.